https://doi.org/10.3311/PPci.22054

Periodica Polytechnica Civil Engineering, 67(3), pp. 795–805, 2023

A New Stress-reduction Model for Soil Arch in Landslides

Xing-ming Li[1], E-chuan Yan[2], Miao Sun[1], Xian-wen Yao[1], Shuo Li[1], Cheng Gao[1], Qian Chen[2*]

[1] College of Environment and Engineering, Hubei Land Resources Vocational College, Wuhan 430090, China
[2] Faculty of Engineering, China University of Geosciences, 430074, Wuhan, China
[*] Corresponding author, e-mail: chenq@cug.edu.cn

Received: 15 February 2023, Accepted: 31 March 2023, Published online: 17 April 2023

Abstract

Stabilizing piles are extensively used as an effective landslide control treatment, and the soil arching effect is the key element for the performance of the pile system. Most previous studies on soil arching effect and its application in stabilizing piles were conducted with laboratory tests and numerical simulations, while limited efforts have been dedicated to the analytical characterization of such a soil-structure interaction. In this paper, a new stress-reduction model for soil arch in landslides is established by theoretical derivation. Our model calculation has demonstrated an exponential reduction in the stress along the direction of slipping between and behind stabilizing piles and thus justifies the observations of laboratory tests and numerical simulations. Thereafter, the analytical solutions to the two key arch shape parameters, namely the inclination angle at the foothold and the thickness of soil arch, are derived based on the proposed stress-reduction model. Then, the ultimate bearing capacity of soil arch between and behind stabilizing piles is subsequently calculated, and a three-level load sharing model for landslides is thus proposed based on the stress-reduction mode. The load sharing model can well capture the stage characteristics of the interaction between landslide mass and stabilizing piles. Finally, the calculation model of spacing between stabilizing piles is established based on the proposed stress-reduction model, and it turns to be good in field application. The findings of this study can contribute to a better understanding of the soil arching effect as well as a better design of the stabilizing piles.

Keywords

soil arching effect, stabilizing piles, stress-reduction model, load sharing model, spacing design

1 Introduction

The stabilizing piles represent one of the most extensively used structures for landslide stabilization worldwide [1–3]. The interaction between each individual stabilizing pile is dictated by soil and pile properties, as well as the level of the soil-induced driving force [4, 5]. Over the past decades, a number of research on the functioning mechanism of stabilizing piles have been carried out by studying the soil arching effect.

The soil arching effect was first reported by Terzaghi [6] through trap-door tests, and its mechanism was further studied and verified by Vardoulakis et al. [7], Low et al. [8], Handy [9], Chevalier et al. [10], Li [11], and George et al. [12]. The soil arching effect is widely used to characterize the interaction between stabilizing piles and surrounding soils with the development [13]. Stress distribution analysis has been a universal method to explain the mechanism of soil arch: experimental studies have shown that the stress in the soil arch changed exponentially [14, 15], and the stress tended to decrease along the direction of the landslide thrust [16]. An alternative approach to characterize soil arch is to examine the force equilibrium between stabilizing piles and surrounding soils [17, 18], and physical models are available for both the soil arches between and behind the stabilizing piles [4] (Fig. 1). As the results, the soil arch shape was built conceptually to better understand the development of soil arch through these research.

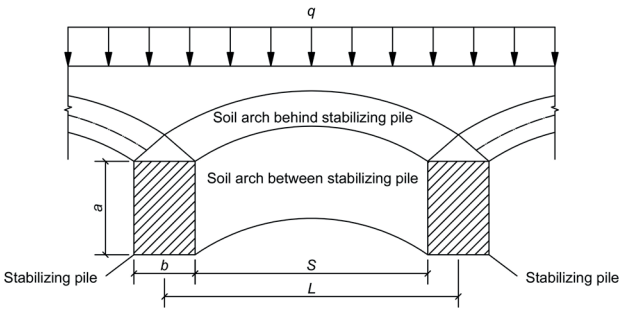

Fig. 1 Interaction between the soil and stabilizing pile system

Cite this article as: Li, X., Yan, E., Sun, M., Yao, X., Li, S., Gao, C., Chen, Q. "A New Stress-reduction Model for Soil Arch in Landslides", Periodica Polytechnica Civil Engineering, 67(3), pp. 795–805, 2023. https://doi.org/10.3311/PPci.22054

However, the value of stress distribution in soil arches has not been described quantitatively and the key parameters of the soil arch shape have not been determined by previous studies.

It is well-known that the movement of a landslide evolves in three well-defined stages [19]. Therefore, the interaction between the soil and stabilizing piles can also exhibit clear transition between each of the three stages as evidenced by the trap-door tests [10, 20]. The three-stage evolution of soil arching effect has also been examined via experimental tests and numerical simulations [11, 21]. These studies showed that to balance the landslide thrust, the soil arch behind stabilizing piles should be mobilized at first, which was then followed by that between stabilizing piles, and finally the soil in front of piles was involved. However, there is currently a lack of rigorous analytical framework that can capture the evolution of soil arching from a mechanistic perspective.

Meanwhile, a number of mathematical models based on the soil arching effect have been proposed for the design of pile spacing [11, 22–25]. Nevertheless, very few have taken the multi-stage and stress-reduction characteristics of the soil arch into account, so the application of those previous models in engineering examples usually does not get the optimal solution. On the other hand, numerical studies of soil arch have also provided valuable insights into the effect of pile spacing on the stress distribution [26–29]. As a result, the law of influence factors on pile spacing has been obtained, however, an analytical model containing the law of these factors is still unavailable. Based on the above two points, a more refined model for pile spacing is needed.

In this paper, a new stress-reduction model for soil arch between and behind stabilizing piles is developed, respectively, and the analytical solutions to the shape parameters of the soil arch are derived based on the proposed model. Then, the stress-reduction model is applied to characterize quantitatively the three-stage evolution of soil arching effect, and a three-level loading sharing model of landslide is thus proposed based on the ultimate bearing capacity of the soil arch. Finally, new methods for determining pile spacing under rectangular and non-rectangular loads are developed based on the stress-reduction model. Application of our model in a recent engineering project shows that the design of pile spacing based on the proposed approach is plausible and has exhibited cost-effectiveness. The present study can contribute to a better understanding of soil arching effect mechanism and practical design of stabilizing piles.

2 A new stress-reduction model for soil arch in landslides

To establish a new stress-reduction model for soil arch, in this section, the axis of soil arch will be determined at first. Then the stress-reduction models for soil arches between and behind stabilizing piles will be established based on Mohr-Coulomb criterion. Finally, the methods for determining the shape parameters of the soil arch are proposed.

2.1 Determination of the axis of soil arch

To characterize the soil arching effect, the axis of soil arch has to be determined at first. The soil arch is commonly considered as a statically determinate structure because it can remain intact under the effect of non-uniform displacements [30]. Assuming that the landslide thrust q is uniformly distributed in the soil between stabilizing piles, for an arbitrary point along the arch axis, there exists only the tangential stress while the tensile stress, shear stress and bending moment all vanishes. As for the force analysis of soil arch shown in Fig. 2, a rectangular coordinate system is established which has its origin at the left arch foothold. The span of arch is l and the height is f. The horizontal and vertical counterforce at arch foothold A and B is denoted by FAx and FAy, and FBx and FBy, respectively.

The mechanical equilibrium of the soil arch ($\sum M_c = 0$, $\sum F_x = 0$, $\sum F_y = 0$) can be expressed as:

$$F_{Ax} f + \frac{1}{8} q l^2 - \frac{1}{2} F_{Ay} l = 0 , \tag{1}$$

$$F_{Ax} - F_{Bx} = 0 , \tag{2}$$

$$F_{Ay} + F_{By} - q l = 0 . \tag{3}$$

One also has $F_{Ay} = F_{By}$ due to the symmetrical nature of the problem. Thus, the counterforce at the arch foothold can be obtained as:

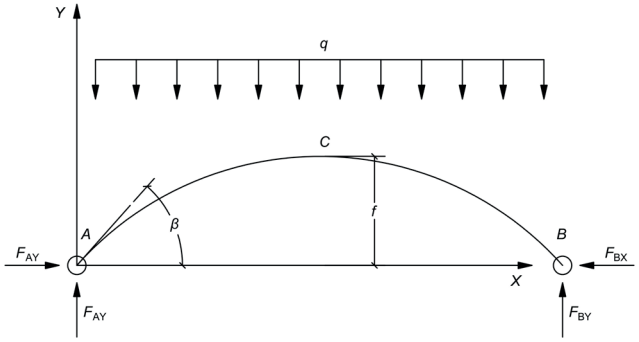

Fig. 2 Mechanical model of soil arch

$$F_x = F_{Ax} = \frac{ql^2}{8f}, \tag{4}$$

$$F_y = F_{Ay} = \frac{1}{2}ql. \tag{5}$$

The angle β between the arch axis and the foothold axis (AB) can be determined as:

$$\tan\beta = \frac{F_y}{F_x} = \frac{4f}{l}. \tag{6}$$

The bending moment of an arbitrary point (x, y) along the arch axis can be expressed as:

$$\sum M(x,y) = F_x y - F_y x + \frac{1}{2}qx^2 = 0. \tag{7}$$

Substituting Eq. (4) and Eq. (5) into Eq. (7) produces the coordinates of the arch axis:

$$y = \frac{4fx(l-x)}{l^2}. \tag{8}$$

Eq. (8) indicates that the arch axis is parabolic under the uniformly distributed thrust induced by landslides, and the shape of the parabolic arch is controlled by its height and span between its footholds.

2.2 Stress-reduction model for soil arch between stabilizing piles

Fig. 3 shows the model for soil arch between stabilizing piles. The width and height of the pile is b and a, respectively. The sliding surface at which the stabilizing piles locate is assumed to be horizontal, while the y axis is assumed to be coincident with the movement direction of the sliding body. The uniformly distributed thrust behind the plies is q_0, the net span between piles is s_0. As shown in Fig. 3, the infinitesimal soil element between the stabilizing piles that has a vertical depth d_h and a thickness d_y is subjected to the thrust of magnitude q and $q + d_q$, respectively.

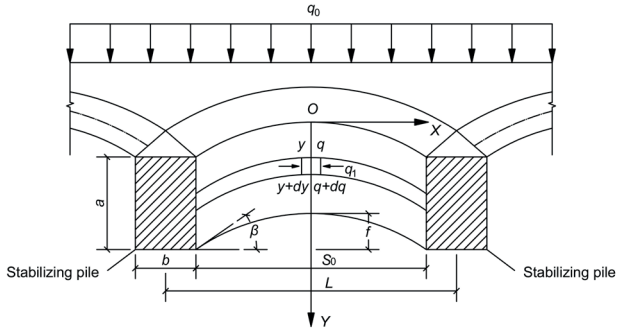

Fig. 3 Model of soil arch between piles

Since $F_y = F_{Ay} = ql/2$, the counterforce of arch foothold acting on the infinitesimal element can be obtained as:

$$dF_y = -\frac{s_0}{2}dq. \tag{9}$$

According to the Mohr-Coulomb criterion, the critical stress in the soil should comply with the following equation:

$$\sigma_1 = \sigma_3 \tan^2\left(45^\circ + \frac{\varphi}{2}\right) + 2c\tan\left(45^\circ + \frac{\varphi}{2}\right). \tag{10}$$

The minor principal stress is $\sigma_3 = q/h$ and Eq. (10) can thus be rewritten as:

$$\sigma_1 = \frac{q}{h}\tan^2\left(45^\circ + \frac{\varphi}{2}\right) + 2c\tan\left(45^\circ + \frac{\varphi}{2}\right), \tag{11}$$

where c denotes cohesion of soil, φ denotes internal friction angle of soil, h denotes thickness of sliding body.

In the middle-section of the soil arch, the horizontal force equals the horizontal component of the supporting force of the arch foothold, which gives:

$$dF_x = \sigma_1 h \cdot dy. \tag{12}$$

To maintain stability of the arch, the soil-pile friction at the interface should not be less than the force imposed by the soil arch between stabilizing piles. At the critical state, one has:

$$Q = N\tan\varphi + clt/\cos\beta, \tag{13}$$

where Q denotes the vertical counterforce on the soil-pile interface per unit depth, N denotes the lateral force that the foothold of the arch imposes on the unit pile depth, t denotes thickness of span, the remaining parameters are the same as above.

Substituting Eq. (9), Eq. (11) and Eq. (12) into Eq. (13) yields:

$$-\frac{s_0}{2}dq = \left[q\tan^2\left(45^\circ + \frac{\varphi}{2}\right) + 2ch\tan\left(45^\circ + \frac{\varphi}{2}\right)\right]\cdot dy\cdot\tan\varphi + \frac{ch}{\cos\beta}dy. \tag{14}$$

Assuming that both the inclination angle β at an arbitrary infinitesimal element and the net spacing s_0 between stabilizing piles remain constant, integration of Eq. (14) thus produces:

$$y = -\frac{s_0}{2k^2\tan\varphi}\ln\left(2k^2\tan\varphi\cdot q + 4chk\tan\varphi + \frac{2ch}{\cos\beta}\right) + D, \tag{15}$$

where $k = \tan(45° + \varphi/2)$, and D is a constant which can be determined when a proper boundary condition is specified. There is $q = q_0$ at $y = 0$, one obtains:

$$y = \frac{s_0}{2k^2 \tan\varphi} \ln\left(\frac{2q_0 k^2 \tan\varphi + 4chk \tan\varphi + \dfrac{2ch}{\cos\beta}}{2qk^2 \tan\varphi + 4chk \tan\varphi + \dfrac{2ch}{\cos\beta}} \right). \quad (16)$$

Eq. (16) can be rewritten in terms of q as:

$$q = (q_0 + \frac{2ch}{k} + \frac{ch}{k^2 \tan\varphi \cos\beta}) e^{-\frac{2k^2 y}{s_0}\tan\varphi} - \frac{2ch}{k} - \frac{ch}{k^2 \tan\varphi \cos\beta}. \quad (17)$$

Upon substituting Eq. (17) into Eq. (11), one has:

$$\begin{aligned} \sigma_1 &= \left[\frac{q_0}{h} k^2 + 2ck + \frac{c}{\tan\varphi \cos\beta} \right] e^{-\frac{2k^2 y \tan\varphi}{s_0}} - \frac{c}{\tan\varphi \cos\beta} \\ &= \left(\sigma_0 + \frac{c}{\tan\varphi \cos\beta} \right) e^{-\frac{2k^2 y \tan\varphi}{s_0}} - \frac{c}{\tan\varphi \cos\beta}. \end{aligned} \quad (18)$$

Eq. (17) and Eq. (18) thus justified the observation of previous laboratory tests and numerical simulations that the landslide thrust as well as the major principal stresses will reduce exponentially along the direction of slipping. Without loss of generality, the soil arch between stabilizing piles should comply with the simplified equation:

$$\sigma = (\sigma_0 + B) e^{Ay} - B, \quad (19)$$

where σ denotes the major principal stress of the arch, $A = \frac{2k^2 \tan\varphi}{s_0}$, $B = \frac{c}{\tan\varphi \cos\beta}$, $y \in [0, t]$, and t denotes the thickness of the soil arch. Eq. (19) represents the stress-reduction model for soil arch between stabilizing piles.

2.3 Stress-reduction model for soil arch behind stabilizing piles

The model for soil arch behind the stabilizing piles is schematically shown in Fig. 4. The hypotenuse of the triangular "soil core" at the arch foothold and the horizontal axis form an angle α. The soil arch is assumed to be subjected to a uniformly distributed thrust q_0.

The span of the infinitesimal element with a thickness dy in the soil arch can be determined by:

$$s = s_0 + b - 2y \cot\alpha. \quad (20)$$

Thus, the height f of the arch can be calculated as:

$$f = \frac{s}{4} \tan\beta = \frac{s}{4} \cdot \frac{4f_0}{s_0} = \frac{f_0}{s_0} (s_0 + b - 2y \cot\alpha) \quad (21)$$

Substituting Eq. (20) and Eq. (21) into Eq. (9) gives the counterforce at the arch foothold:

$$dF_y = -\frac{s_0 + b - 2y \cot\alpha}{2} dq. \quad (22)$$

The static equilibrium of the soil arch behind the piles requires that the sum of the piles' lateral friction should be no less than the thrust that is imposed on the soil arch between the piles. Therefore, substituting Eq. (13) into Eq. (22) then yields:

$$-\frac{s_0 + b - 2y \cot\alpha}{2} dq = \left[qk^2 + 2chk \right] dy \cdot \tan\varphi + \frac{ch}{\cos\beta} dy \quad (23)$$

Considering the boundary condition that $q = q_0$ at $y = 0$, integration of Eq. (23) thus produces:

$$y = \frac{s_0 + b}{2} \tan\alpha \cdot \left\{ 1 - \left[\frac{qk + 2ch + \dfrac{ch}{k \tan\varphi \cos\beta}}{q_0 k + 2ch + \dfrac{ch}{k \tan\varphi \cos\beta}} \right]^{\frac{1}{k^2 \tan\alpha \tan\varphi}} \right\} \quad (24)$$

Eq. (24) can be rewritten in terms of q as:

$$q = \left(q_0 + \frac{2ch}{k} + \frac{ch}{k^2 \tan\varphi \cos\beta} \right) \cdot \left[1 - \frac{2y}{(s_0 + b) \tan\alpha} \right]^{k^2 \tan\alpha \tan\varphi} - \frac{2ch}{k} - \frac{ch}{k^2 \tan\varphi \cos\beta}. \quad (25)$$

Substituting Eq. (25) into Eq. (11), one obtains:

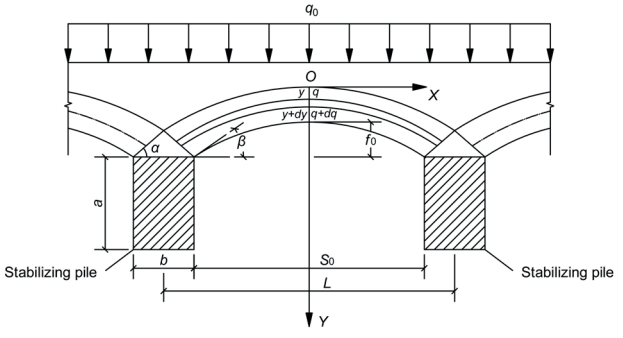

Fig. 4 Model for soil arch behind piles

$$\sigma_1 = \left(\frac{q_0}{h}k^2 + 2ck + \frac{c}{\tan\varphi\cos\beta}\right)\times \left[1 - \frac{2y}{(s_0 + b)\tan\alpha}\right]^{k^2\tan\alpha\tan\varphi} - \frac{c}{\tan\varphi\cos\beta}. \quad (26)$$

Which can also be simplified as:

$$\sigma_1 = (\sigma_0 + B)\left[1 - \frac{2y}{(s_0 + b)\tan\alpha}\right]^{k^2\tan\alpha\tan\varphi} - B, \quad (27)$$

where $B = c/(\tan\varphi\cos\beta)$. Because the earth pressure in the triangular soil core is passive, it is thus considered to be in an elastic state with a failure angle $\alpha = 45° + \varphi/2$. Eq. (25) and Eq. (27) also prove mathematically that both the landslide thrust and the stress of the soil arch behind piles exhibit an exponential reduction along the direction of slipping, in good agreement with the findings of previous laboratory tests and numerical simulations. Eq. (27) represents the stress-reduction model for soil arch behind piles.

2.4 Determination of shape parameters of the soil arch

While the existence of soil arching effect has been proven through earlier experimental tests and numerical simulations, most of these studies have focused on a qualitative description of the soil arch evolution, and very few models are available for defining the shape parameters of soil arch quantitatively. If a model can be used to define the shape parameters of soil arch, it will be helpful to understand the soil arching effect more clearly. In this section, analytical solutions to the shape parameters of the soil arch are derived based on the stress-reduction model developed. Besides, the key problem usually forces on the height and the thickness of soil arch because the span of soil arch and the position of arch footholds are relatively specified. Therefore, we will give the calculation methods of the height and the thickness.

2.4.1 The shape parameters of soil arch between stabilizing piles

The counterforce at the arch foothold can be determined from Eq. (4) as:

$$dF_x = -\frac{s_0^2}{8f}dq. \quad (28)$$

Substitution of Eq. (11) and Eq. (28) into Eq. (12) gives:

$$-\frac{s_0^2}{8f}\frac{dq}{dy} = q\tan^2\left(45^\circ + \frac{\varphi}{2}\right) + 2ch\tan\left(45^\circ + \frac{\varphi}{2}\right). \quad (29)$$

Eq. (29) can be further substituted into Eq. (14) to obtain:

$$\frac{4f}{s_0} = \tan\varphi + \frac{ch}{\left(q\tan^2\left(45^\circ + \frac{\varphi}{2}\right) + 2ch\tan\left(45^\circ + \frac{\varphi}{2}\right)\right)\cos\beta}. \quad (30)$$

Noting that $\tan\beta = 4f/s$, then Eq. (30) can be rewritten as:

$$\tan\beta = \tan\varphi + \frac{ch}{\left[q\tan^2\left(45^\circ + \frac{\varphi}{2}\right) + 2ch\tan\left(45^\circ + \frac{\varphi}{2}\right)\right]\cos\beta}. \quad (31)$$

The solution to β can thus be obtained as:

$$\beta = \varphi + \arcsin\left(\frac{ch\cos\varphi}{qk^2 + 2chk}\right). \quad (32)$$

Eq. (32) indicates that the inclination angle β of soil arch at the foothold is related to the landslide thrust. At present, there are three methods for determining β based on the internal friction angle of soil: φ, $45 + \varphi/2$, $45 - \varphi/2$. However, these methods have not considered the landslide thrust and cohesion force, so a model that consider the landslide thrust and cohesion force is required. In this study, we suggest that the incline angle β is considered equal to the incline angle of the arch axis at the trailing edge of the soil arch. For elements at $y = 0$ under a landslide thrust q_0, β can be determined as:

$$\beta = \varphi + \arcsin\left(\frac{ch\cos\varphi}{q_0k^2 + 2chk}\right). \quad (33)$$

Therefore, the incline angle β determined via Eq. (33) has taken both the strength parameters of soil and landslide thrust into account, which is more realistic because the existing methods have only considered the effect of internal friction angle φ.

The incline angle β can be further inserted into Eq. (6) to determine the arch height f. Finally, upon substituting f into Eq. (18), the stress-reduction model for soil arch between stabilizing piles is completed.

Due to the constraint brought by the size of the pile section, there is a maximum thickness for the soil arch between piles, which is determined by the height a and the incline angle β. According to Fig. 3, the maximum thickness of soil arch between piles can be determined as:

$$t_{\max} = a\cos\beta \ . \tag{34}$$

When $t < t_{\max}$ (i.e., the thickness of the soil arch between piles is less than its maximum capacity), the landslide thrust sustained at the bottom edge of the soil arch is zero. The thickness of the arch can thus be determined at the location where $q = 0$, from Eq. (16) as:

$$t = \frac{s_0}{2k^2\tan\varphi}\ln\left(\frac{q_0k^2}{2chk+\dfrac{ch}{\tan\varphi\cos\beta}}+1\right). \tag{35}$$

If the thickness t calculated from Eq. (35) is greater than $t_{\max}$, the landslide thrust would exceed the ultimate bearing capacity of the soil arch and a part of load would be directly imposed on the sliding body.

2.4.2 The shape parameters of soil arch behind stabilizing piles

The soil arch between and behind stabilizing piles differs from each other in that the span s of the soil arch behind piles is variable while the other is not. For an infinitesimal element with a thickness of *dy* in the soil arch behind stabilizing piles, substitution of Eq. (20) and Eq. (21) into Eq. (4) gives the foothold counterforce *dFx*:

$$dF_x = -\frac{s_0^2}{8f}dq = -\frac{s_0\left(s_0+b-2y\cot\alpha\right)}{8f_0}dq \ . \tag{36}$$

Finally, substituting Eq. (11) and Eq. (36) into Eq. (12) yields the differential equation for the infinitesimal soil element behind stabilizing piles:

$$\begin{aligned}&-\frac{s_0\left(s_0+b-2y\cot\alpha\right)}{8f_0}dq\\&=\left[q\tan^2\left(45^\circ+\frac{\varphi}{2}\right)+2ch\tan\left(45^\circ+\frac{\varphi}{2}\right)\right]dy.\end{aligned} \tag{37}$$

Noticing that $\tan\beta = 4f_0/s_0$, combination of Eq. (37) and Eq. (23) thus produces:

$$\tan\beta = \tan\varphi + \frac{ch}{\left(q\tan^2\left(45^\circ+\dfrac{\varphi}{2}\right)+2ch\tan\left(45^\circ+\varphi\right)\right)\cos\beta}. \tag{38}$$

We can see that Eq. (38) is the same as Eq. (31) in form, so the result of value will be the same in form, and the value of inclination angle β for soil arch behind piles can be also calculated by Eq. (33).

The incline angle β can be further inserted into Eq. (6) to determine the arch height *f*, and thus completes the stress-reduction model for soil arch behind stabilizing piles upon substitution of *f* into Eq. (26).

Owing to the constraint brought by the size of the pile section, there is also a maximum thickness for the soil arch behind piles. According to Fig. 4, the maximum thickness can be determined as:

$$t_{\max} = \frac{b\sin\left(\pi-\alpha-\beta\right)}{2\cos\alpha} = \frac{b\sin\left(\alpha+\beta\right)}{2\cos\alpha} \ . \tag{39}$$

Similarly, the maximum range of the soil arch behind stabilizing piles is not yet reached when $t < t_{\max}$. Thus, the landslide thrust sustained at the bottom edge of the soil arch equals zero. The thickness of the arch can thus be determined at the location where $q = 0$. According to Eq. (24), it has:

$$t = \frac{s_0+b}{2}\tan\alpha\cdot\left\{1-\left[\frac{2ch+\dfrac{ch}{k\tan\varphi\cos\beta}}{q_0k+2ch+\dfrac{ch}{k\tan\varphi\cos\beta}}\right]^{\frac{1}{k^2\tan\alpha\tan\varphi}}\right\} \tag{40}$$

If $t > t_{\max}$, the landslide thrust would exceed the maximum bearing capacity of the soil arch and a part of load would be directly imposed on the soil arch between piles.

3 Three-level load sharing model for landslides

3.1 Derivation of three-stage model for soil–pile interaction

The load distribution in landslides is directly related to the characteristics of the interaction between the soil and stabilizing piles. Extensive research works have been dedicated to the soil arching effect since it was first observed in the trap-door test by Terzaghi [6]. Vardoulakis et al. [7] proposed the concept of "transitory stage" for soil arching effect and it was verified recently by Spangler [31], Ladanyi and Hoyaux [32], Chevalier et al. [10, 20], and Rui et al. [33]. These studies indicated that the trap-door test consists of three stages: (a) the initial stage: as the granular material above the trap door dilates, this stage will last before the vertical load above the trap-door decreases to its minimum (the displacement is 1 mm~3 mm); (b) the transitory stage: the dilatancy area formed above the trap door keeps expanding till it reaches the soil surface, and the dilatancy area will be in a wedge shape (the displacement is 3 mm~40 mm); (c) the final stage: in this stage two vertical slipping surfaces will be formed (the displacement is 40 mm~100 mm).

The different stages of the trap-door test are shown in Fig. 5.

The three stages revealed the trap-door test suggested that the soil arch exhibits obvious evolutive characteristics, which are influenced by the width of the trap door, the depth and the properties of soil, etc. Moreover, the soil arch that emerged during the transitory stage is normally considered as the arch of minor principal stress, whereas the arch of major principal stress is considered to emerge during the last stage [9].

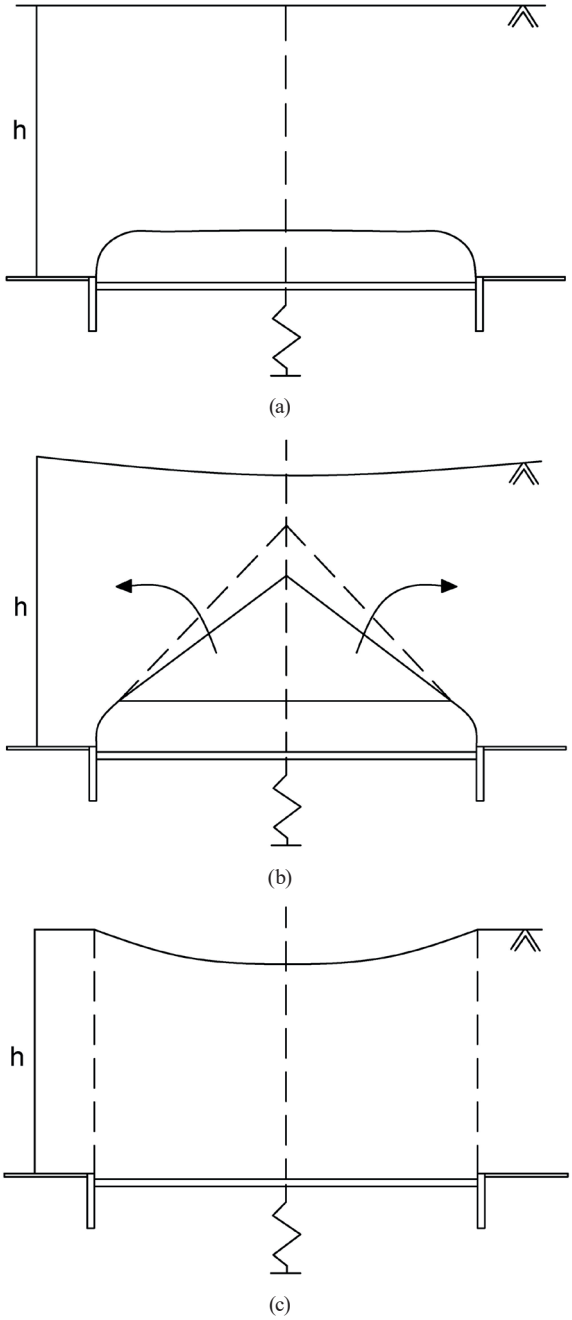

Fig. 5 Three-stage of the trap-door test; (a) Initial stage, (b) Transitory stage, (c) Final stage

Similar to the soil arch development in the trap-door test, the soil arching effect resulting from the interaction between soil and stabilizing piles should also exhibit a three-stage evolution, and it should be relevant to the space between piles, the depth of the sliding body and the mechanical parameters. Arch of the minor principal stress should emerge in the transitory stage during the interaction between soil and stabilizing piles, and the soil arch behind stabilizing piles is thus mobilized firstly and plays the dominant role. Then, arch of the major principal stress emerges in the last stage and the soil arch between stabilizing piles plays the dominant role.

According to the proposed stress-reduction model, the stress distribution in the soil arch behind piles during the transitory stage can be determined by Eq. (26), and the stress is affected by b, α, q_0, h, c and φ. In the final stage, the stress distribution in soil arch between piles can be characterized by Eq. (18), while the stress is no longer affected by b and α. At the same time, considering the continuity of Fig. 5(b) to 5(c) for the trap-door test, a typical phenomenon of stages altering is thought to be the gradual increment of the angle formed by horizontal line and the dilatancy fracture zone. And when the fracture angle increases toward 90° the test will be altered from transitory stage to final stage. Therefore, the influencing factors of soil arch in different stress-reduction models coincide with the evolution process from transitory stage to final stage.

Based on the analysis above, apparent changes during the interaction between soil and stabilizing piles from transitory stage to final stage can be summarized: The first is the effect of soil arch between piles plays an increasingly important role compared to that behind the piles; the second is the angle α, the hypotenuse of the triangular soil core and horizontal line, increases towards 90°, and the width b of the stabilizing pile's section will gradually become less effective. Therefore, for soil arch behind piles, if Eq. (26) gives the limitation of σ_1 by letting $b = 0$ and $\alpha = 90°$, then Eq. (26) would become Eq. (41):

$$\lim_{\substack{\alpha\to 90^{-}\\ b=0}} \sigma_1 = \lim_{\substack{\alpha\to 90^{-}\\ b=0}} \left(\sigma_0 + B\right)\left[1 - \frac{2y}{\left(s_0 + b\right)\tan\alpha}\right]^{k^2 \tan\alpha \tan\varphi} - B = \left(\sigma_0 + B\right) e^{-\frac{2k^2 y \tan\varphi}{s_0}} - B. \tag{41}$$

Consistent with the conclusions of test inference, Eq. (41) deduces numerically the evolution process from the transitory stage to the final stage of the interaction between the soil and the stabilizing piles, verifies the

rationality of the three-stage model of the trap-door test, and also illustrates the validity and correctness of stress-reduction model for soil arch.

3.2 Three-level load sharing model for landslide

During the three-stage interaction evolution, the effects of soil arch behind and between the piles contributes differently to the earth pressure distribution in the different stages. In this section, the ultimate bearing capacity of the soil arches behind and between piles will be deduced and the load sharing model of landslide will also be proposed based on the stress-reduction model of soil arch.

(1) Ultimate bearing capacity of soil arch behind piles

Solving q_0 from Eq. (25) gives:

$$q_0 = \left(q + \frac{2ch}{k} + \frac{ch}{k^2 \tan\varphi \cos\beta} \right) \cdot \left[1 - \frac{2y}{\left(s_0 + b \right) \tan\alpha} \right]^{-k^2 \tan\alpha \tan\varphi} - \frac{2ch}{k} - \frac{ch}{k^2 \tan\varphi \cos\beta}. \tag{42}$$

Upon reaching the ultimate bearing capacity, the thickness of the soil arch behind piles maximizes. Substituting $q = 0$, and $y = t_{\max}$ into Eq. (42), one obtains:

$$q_0 = \left[\frac{2ch}{k} + \frac{ch}{k^2 \tan\varphi \cos\beta} \right] \cdot \left[1 - \frac{b \sin\left(\alpha + \beta \right)}{\left(s_0 + b \right) \sin\alpha} \right]^{-k^2 \tan\alpha \tan\varphi} - \frac{2ch}{k} - \frac{ch}{k^2 \tan\varphi \cos\beta}, \tag{43}$$

which represents the analytical solution to the maximum landslide thrust sustained by the soil arch behind piles.

(2) The ultimate bearing capacity of soil arch between piles

Solving q_0 from Eq. (17) gives:

$$q_0 = \left(q + \frac{2ch}{k} + \frac{ch}{k^2 \tan\varphi \cos\beta} \right) e^{\frac{2k^2 y}{s_0} \tan\varphi} - \frac{2ch}{k} - \frac{ch}{k^2 \tan\varphi \cos\beta}. \tag{44}$$

Substitution of the boundary condition $q = 0$ at $y = 0$ into Eq. (44) gives:

$$q_0 = \left(\frac{2ch}{k} + \frac{ch}{k^2 \tan\varphi \cos\beta} \right) e^{\frac{2k^2 a \cos\beta}{s_0} \tan\varphi} - \frac{2ch}{k} - \frac{ch}{k^2 \tan\varphi \cos\beta}, \tag{45}$$

which represents the analytical solution to the maximum landslide thrust sustained by the soil arch between piles.

(3) Three-level loading sharing model for landslide

Assuming that the ultimate bearing capacity of the soil arch behind and between the stabilizing piles is q_1 and q_2, respectively, the three-level load sharing model for landslide can be built based on the soil arching effect. When the landslide thrust $q < q_1$, the thrust is sustained mainly by soil arch behind piles, and the interaction between soil and stabilizing piles remains in the transitory stage. When the landslide thrust lies between the ultimate bearing capacities of those two limiting conditions, (i.e., $q_1 < q < q_2$), the thrust is sustained mostly by soil arch between piles, and the interaction between soil and stabilizing piles is at the final stage. When the landslide thrust $q > q_2$, the soil arching effect vanishes as the piles destabilize, and the landslide thrust is borne by the back wall of stabilizing piles and the soil in front.

This three-level load sharing model for landslide proposed in this paper has the following advantages: First, it has evolved different stages of pile-soil interaction from two aspects: landslide load and soil arching effect; second, it quantifies the stress distribution value and analyzes the key factors of the soil arch at different stages; third, it quantifies the three-level load sharing model of landslide, which is consistent with the characteristics of different stages during the interaction between soil and stabilizing piles.

4 Design of pile spacing and engineering application

The relationship between pile spacing s and net pile spacing s_0 can be expressed as:

$$s = s_0 + b. \tag{46}$$

Based on the proposed three-level load sharing model for landslides, the minimum pile spacing denotes the spacing that permits the landslide thrust to be resisted solely by the soil arching effect behind piles. If the designed pile spacing was less than the minimum value, the layout of stabilizing piles could be too conservative to exploit the soil arching effect. On the other hand, the maximum pile spacing dictates the spacing that allows the landslide thrust to be borne by the arching effect between piles alone. If the designed pile spacing was greater than the maximum value, the design could be insecure.

In this section, design models for critical pile spacing under rectangular and non- rectangular landslide thrusts will be developed. Their successful application to a recent landslide control project will be also presented.

4.1 Critical pile spacing under rectangular landslide thrust

If the distribution of the landslide thrust along the length of pile has a rectangular form, one can combine Eq. (33), Eq. (43) and Eq. (46) to obtain the minimum pile spacing based on the model for the soil arch behind piles:

$$s_{min} = \frac{b\sin(\alpha+\beta)}{\left[1-\left(\frac{2ch+\frac{ch}{k\tan\varphi\cos\beta}}{q_0k+2ch+\frac{ch}{k\tan\varphi\cos\beta}}\right)^{\frac{1}{k^2\tan\alpha\tan\varphi}}\right]\cdot\sin\alpha}. \tag{47}$$

Similarly, combination of Eq. (33), Eq. (35) and Eq. (46) can provide the maximum pile spacing based on the model for soil arch between piles:

$$s_{max} = 2k^2a\cos\beta\tan\varphi\cdot\ln^{-1}\left[\frac{q_0k+2ch+\frac{ch}{k\tan\varphi\cos\beta}}{2ch+\frac{ch}{k\tan\varphi\cos\beta}}\right]+b. \tag{48}$$

4.2 Critical pile spacing under non-rectangular load

Generally, the landslide thrust can distribute in a rectangular, trapezoid or triangular form along the length of a stabilizing pile. Assuming that the landslide thrust that distributes along the length of a stabilizing pile is $q(z)$, we can define the distributive ratio η of landslide thrust as the ratio of its maximum value q_{max} to its mean value q as:

$$\eta = \frac{q_{max}}{\overline{q}} = q_{max}\Big/\left(\frac{\int_0^Z q(z)\,dz}{Z}\right). \tag{49}$$

It is apparent from Eq. (49) that for rectangular load, $\eta = 1$; for triangular load, $\eta = 2$; and for trapezoid load, $1 < \eta < 2$.

Considering the non-uniformity of the landslide thrust distribution along the pile depth, the pile spacing should be determined by the stability of the most unfavorable soil arch where the maximum landslide thrust lies. Thus, the equation for pile spacing under rectangular load should be corrected by the distributive ratio of landslide thrust.

Substituting Eq. (49) into Eq. (33), the corrected inclination angle β can be expressed as:

$$\beta = \varphi + \arcsin\left(\frac{ch\cos\varphi}{\eta q_0k^2+2chk}\right). \tag{50}$$

Then, by substituting Eq. (49) into Eq. (47), the corrected minimum pile spacing based on the soil arch behind piles can thus be determined as:

$$s_{min} = \frac{b\sin(\alpha+\beta)}{\left[1-\left(\frac{2ch+\frac{ch}{k\tan\varphi\cos\beta}}{\eta q_0k+2ch+\frac{ch}{k\tan\varphi\cos\beta}}\right)^{\frac{1}{k^2\tan\alpha\tan\varphi}}\right]\cdot\sin\alpha}. \tag{51}$$

Similarly, the maximum pile spacing based on the soil arch between piles after correction can be rewritten as:

$$s_{max} = 2k^2a\cos\beta\tan\varphi\cdot\ln^{-1}\left[\frac{\eta q_0k+2ch+\frac{ch}{k\tan\varphi\cos\beta}}{2ch+\frac{ch}{k\tan\varphi\cos\beta}}\right]+b. \tag{52}$$

4.3 Application to engineering practice

A soil landslide in Ganluo County of western Sichuan, China, employed stabilizing piles for instability mitigation. The cohesion of the landslide material was $c = 27$ kPa, and the internal friction angle was $\varphi = 16°$. Calculations showed that the maximum landslide thrust near the arch axis was $q_0 = 1240$ kN/m, the loading section of stabilizing pile was 14 m in length, and the designed width and height of the pile section was $b = 2$ m and $a = 3$ m, respectively. The landslide thrust was considered to be in a rectangular form. There are several pile design methods based on different models of soil arching effect, the results of pile spacing according to the various design models are as follows:

Table 1 showed that pile spacing obtained from Zhou's model was significantly smaller than those from others'. This is probably because the soil in the front of stabilizing piles and the pile height were not incorporated in

Table 1 Results of pile spacing

Method	Wang [23]	Zhou [24]	Zhao [25]	Li [11]	This paper
model	Arch between piles	Arch behind piles	Arch between piles	Arch between piles	Arch between piles
result	4.56 m	3.17 m	4.33 m	4.61 m	5.51 m

Zhou et al. [24]. The other models have also provided lower pile spacing than that determined by the proposed approach in this paper. The differences can be attributed to the fact that these models did not take the stress-reduction characteristic of soil arch into account and thus the bearing capacity of soil arch was underestimated. The proposed method in this paper is obviously reasonable and more economically beneficial. For a designed factor of safety of 1.35, the proposed model suggests that the maximum spacing between piles is 4.08 m, and a spacing of 4.0 m was adopted in this prevention measure for the landslide. The landslide has remained stable since 2013 by adopting the layout of the stabilizing piles suggested by the proposed method.

5 Conclusions

A new stress-reduction model is developed in this paper to better understand the soil arching effect under the interaction between soil and stabilizing piles. The stress-reduction model shows that the stress of soil arch between and behind stabilizing piles decreases exponentially. Based on the stress-reduction model, the shape parameter formulas of soil arch are proposed, which comprehensively consider the influence of soil strength parameters and landslide thrust, and describe the shape of soil arch more precisely.

The evolution process of stress-reduction model from soil arch behind piles to soil arch between piles is derived numerically, which proves that the three-stage theory of soil arching effect in landslide is reasonable. It suggested that as the soil arching effect in landslide evolves from the transitory stage to the final stage, the controlling mechanism changes from the soil arch behind stabilizing piles to the soil arch between the stabilizing piles. Meanwhile, when angle α formed by the hypotenuse of the triangular soil core and horizontal line, increased to 90°, the section width of stabilizing piles becomes increasingly less significant. By determining the ultimate bearing capacity of soil arch behind and between stabilizing piles, a new three-level load sharing model of landslide is proposed, which has a positive meaning for understanding the evolution of interaction between soil and stabilizing pile.

The load distributive ratio is proposed, and the calculation models of pile spacing under rectangular and non-rectangular loads are derived respectively by using the stress-reduction model. The models of pile spacing fully consider both characteristics of different stages and characteristics of stress-reduction under soil arching effect. Compared with other models in the engineering example, the calculation model in the paper is more reasonable and more economical. The research has positive significance for the advancement of soil arching effect theory and the design of practical stabilizing pile engineering.

Acknowledgements

This research was supported by National Natural Science Foundation of China (No. 41672313), and National Natural Science Foundation of China (No. 41972289), and Engineering Research Center of Rock-Soil Drilling & Excavation and Protection, Ministry of Education.

References

[1] Poulos, H. G. "Design of reinforcing piles to increase slope stability", Canadian Geotechnical Journal, 32(5), pp. 808–818, 1995. https://doi.org/10.1139/t95-078

[2] Wang, G., Sassa, K. "Pore-pressure generation and movement of rainfall-induced landslides: Effects of grain size and fine-particle content", Engineering Geology, 69(1–2), pp. 109–125, 2003. https://doi.org/10.1016/S0013-7952(02)00268-5

[3] Tang, H., Hu, X., Xu, C., Li, C., Yong, R., Wang, L. "A novel approach for determining landslide pushing force based on landslide-pile interactions", Engineering Geology, 182, pp. 15–24, 2014. https://doi.org/10.1016/j.enggeo.2014.07.024

[4] Ashour, M., Ardalan, H. "Analysis of pile stabilized slopes based on soil-pile interaction", Computers and Geotechnics, 35, pp. 85–97, 2012. https://doi.org/10.1016/j.compgeo.2011.09.001

[5] Li, C., Wu, J., Tang, H., Wang, J., Chen, F., Liang, D. "A novel optimal plane arrangement of stabilizing piles based on soil arching effect and stability limit for 3D colluvial landslides", Engineering Geology, 195, pp. 236–247, 2015. https://doi.org/10.1016/j.enggeo.2015.06.018

[6] Terzaghi, K. "Retaining Wall Problems", In: Theoretical Soil Mechanics, John Wiley & Sons, 1943, pp. 76–85. ISBN: 978-0471853053 https://doi.org/10.1002/9780470172766

[7] Vardoulakis, I., Graf, B., Gudehus, G. "Trap-door problem with dry sand: A statical approach based upon model test kinematics", International Journal for Numerical and Analytical Methods in Geomechanics, 5(1), pp. 57–78, 1981. https://doi.org/10.1002/nag.1610050106

[8] Low, B. K., Tang, S. K., Choa, V. "Arching in Piled Embankments", Journal of Geotechnical Engineering, 120(11), pp. 1917–1937, 1994. https://doi.org/10.1061/(asce)0733-9410(1994)120:11(1917)

[9] Handy, R. L. "The Arch in Soil Arching", Journal of Geotechnical Engineering, 111(3), pp. 302–318, 1985. https://doi.org/10.1061/(asce)0733-9410(1985)111:3(302)

[10] Chevalier, B., Combe, G., Villard, P. "Experimental and numerical study of the response of granular layer in the trap-door problem", AIP Conference Proceedings, 1145, pp. 649–652, 2009. https://doi.org/10.1063/1.3180010

[11] Li, C. D. "Study on Interaction Mechanism Between Anti-slide Pile and Landslide Mass and Pile Optimization", PhD Thesis, China University of Geosciences, 2009. (in Chinese) [online] Available at: https://www.ckcest.cn/default/es3/detail/1003/dw_thesis_copy/1043834

[12] George T. I., Dasaka S. M. "Mechanics of arch action in soil arching", Acta Geotechnica, 2022. https://doi.org/10.1007/s11440-022-01697-0

[13] Chen, C.-Y., Martin, G. R. "Soil-Structure interaction for landslide stabilizing piles", Computers and Geotechnics, 29(5), pp. 363–386, 2002. https://doi.org/10.1016/S0266-352X(01)00035-0

[14] Janssen, H. A. "Versuche uber getreidedruck in Silozellen" (Experiments on corn pressure in silo cells), Zeitschrift des Vereines Deutscher Ingenieure, 39, pp. 1045–1049, 1895. (in German)

[15] Zheng, X.X. "Analysis and simulation of soil arching effects on anti-slide piles", MSc Thesis, Hohai University, 2007. (in Chinese) [online] Available at: https://www.dissertationtopic.net/doc/1111138

[16] Zhang J. X., Chen F. Q., Jian H. Y. "Numerical analysis of soil arching effects in passive piles", Rock and Soil Mechanics, 25(2), pp. 174–178, 2004. (in Chinese) https://doi.org/10.3969/j.issn.1000-7598.2004.02.002

[17] Ashour, M., Norris, G. "Modeling Lateral Soil-Pile Response Based on Soil-Pile Interaction", Journal of Geotechnical and Geoenvironmental Engineering, 126(5), pp. 420–428, 2000. https://doi.org/10.1061/(asce)1090-0241(2000)126:5(420)

[18] Tomio, I., Tamotsu, M. "Methods to estimate lateral force acting on stabilizing piles", Soils and Foundations, 15(4), pp. 43–59, 1975. https://doi.org/10.3208/sandf1972.15.4_43

[19] Ma, J.-W., Tang, H.-M., Hu, X.-L., Yong, R., Xia, H., Song, Y.-J. "Application of 3D laser scanning technology to landslide physical model test", Rock and Soil Mechanics, 35(5), pp. 1495–1505, 2014. (in Chinese) https://doi.org/10.16285/j.rsm.2014.05.002

[20] Chevalier, B., Combe, G., Villard, P. "Load transfers and arching effects in granular soil layer", In: 18ème Congrès Français de Mécanique, Grenoble, France, 2007, pp. 27–31. [online] Available at: https://www.researchgate.net/publication/27610314

[21] Li, C., Tang, H., Hu, X., Wang, L. "Numerical modelling study of the load sharing law of anti-sliding piles based on the soil arching effect for Erliban landslide, China", KSCE Journal of Civil Engineering, 17(6), pp. 1251–1262, 2013. https://doi.org/10.1007/s12205-013-0074-x

[22] Ito, T., Matsui, T. "Methods to Estimate Lateral Force Acting on Stabilizing Piles", Soils and Foundations, 15(4), pp. 43–59, 1975. https://doi.org/10.3208/sandf1972.15.4_43

[23] Wang, C.-H., Chen, Y.-B., Lin, L.-X. "Soil arch mechanical character and suitable space between one another anti-sliding pile", Journal of Mountain Science, 19(6), pp. 556–559, 2001. (in Chinese) https://doi.org/10.3969/j.issn.1008-2786.2001.06.013

[24] Zhou, P.-D., Xiao, S.-G., Xia, X. "Discussion on rational spacing between adjacent anti-slide piles in some cutting slope projects", Chinese Journal of Geotechnical Engineering, 26(1), pp. 132–135, 2004. (in Chinese) https://doi.org/10.3321/j.issn:1000-4548.2004.01.025

[25] Zhao, M.-H., Chen, B.-C., Liu, J.-H. "Analysis of the spacing between anti-slide piles considering soil-arch effect", Central South Highway Engineering, 32(2), pp. 1–3, 2006. (in Chinese) https://doi.org/10.3969/j.issn.1674-0610.2006.02.001

[26] Won, J., You, K., Jeong, S., Kim, S. "Coupled effects in stability analysis of pile-slope systems", Computers and Geotechnics, 32(4), pp. 304–315, 2005. https://doi.org/10.1016/j.compgeo.2005.02.006

[27] Fan, C.-C., Long, J. H. "Assessment of existing methods for predicting soil response of laterally loaded piles in sand", Computers and Geotechnics, 32(4), pp. 274–289, 2005. https://doi.org/10.1016/j.compgeo.2005.02.004

[28] Ellis, E. A., Durrani, I. K., Reddish, D. J. "Numerical modelling of discrete pile rows for slope stability and generic guidance for design", Géotechnique, 60(3), pp. 185–195, 2010. https://doi.org/10.1680/geot.7.00090

[29] Lirer, S. "Landslide stabilizing piles: Experimental evidences and numerical interpretation", Engineering Geology, 149–150, pp. 70–77, 2012. https://doi.org/10.1016/j.enggeo.2012.08.002

[30] Jia, H.-L. "Discussion on Some Issues in Theory of Soil Arch", Journal of Southewest Jiaotong University, 38(4), pp. 398–402, 2003. (in Chinese) https://doi.org/10.3969/j.issn.0258-2724.2003.04.007

[31] Spangler, M. G. "Section 11: Culverts and conduits", In: Leonard, G. A. (ed.) Foundation Engineering, McGraw-Hill, 1962, pp. 965–999. ISBN: 0070371989

[32] Ladanyi, B., Hoyaux, B. "A study of the trap-door problem in a granular mass", Canadian Geotechnical Journal, 6(1), pp. 1–14, 1969. https://doi.org/10.1139/t69-001

[33] Rui, R., van Tol, A., Xia, Y., van Eekelen, S., Hu, G. "Investigation of soil-arching development in dense sand by 2D model tests", Geotechnical Testing Journal, 39(3), pp. 415–430, 2016. https://doi.org/10.1520/GTJ20150130